

The Hubble flow around the Cen A/M 83 galaxy complex

Igor D. Karachentsev

Special Astrophysical Observatory, Russian Academy of Sciences, N. Arkhyz, KChR,
369167, Russia

ikar@luna.sao.ru

R. Brent Tully

Institute for Astronomy, University of Hawaii, Honolulu, HI 96822

Andrew Dolphin

Steward Observatory, 933 N. Cherry Ave., Tucson, AZ 85721

Margarita Sharina, Lidia Makarova^{1,2} and Dmitry Makarov^{1,2}

Special Astrophysical Observatory, Russian Academy of Sciences, N. Arkhyz, KChR,
369167, Russia

Shoko Sakai

Division of Astronomy and Astrophysics, University of California, at Los Angeles, Los
Angeles, CA 90095-1562

Edward J. Shaya

Astronomy Department, University of Maryland, College Park, MD 20743

Olga G. Kashibadze

Moscow State University

Valentina Karachentseva

Astronomical Observatory of Kiev University, Kiev 04053, Ukraine

Luca Rizzi

Institute for Astronomy, University of Hawaii, Honolulu, HI 96822

Received _____; accepted _____

¹also Institute for Astronomy, University of Hawaii, 2680 Woodlawn Drive, Honolulu, HI 96822

²Isaac Newton Institute of Chile, SAO Branch

ABSTRACT

We present HST/ACS images and color-magnitude diagrams for 24 nearby galaxies in and near the constellation of Centaurus with radial velocities $V_{LG} < 550 \text{ km s}^{-1}$. Distances are determined based on the luminosities of stars at the tip of the red giant branch that range from 3.0 Mpc to 6.5 Mpc. The galaxies are concentrated in two spatially separated groups around Cen A (NGC 5128) and M 83 (NGC 5236). The Cen A group itself has a mean distance of 3.76 ± 0.05 Mpc, a velocity dispersion of 136 km s^{-1} , a mean harmonic radius of 192 kpc, and an estimated orbital/virial mass of $(6.4 - 8.1) \cdot 10^{12} M_{\odot}$. This elliptical dominated group is found to have a relatively high mass-to-light ratio: $M/L_B = 125 M_{\odot}/L_{\odot}$. For the M 83 group we derived a mean distance of 4.79 ± 0.10 Mpc, a velocity dispersion of 61 km s^{-1} , a mean harmonic radius of 89 kpc, and estimated orbital/virial mass of $(0.8 - 0.9) \cdot 10^{12} M_{\odot}$. This spiral dominated group is found to have a relatively low $M/L_B = 34 M_{\odot}/L_{\odot}$. The radius of the zero-velocity surface around Cen A lies at $R_0 = 1.40 \pm 0.11$ Mpc. implying a total mass within R_0 of $M_T = (6.0 \pm 1.4) \cdot 10^{12} M_{\odot}$. This value is in good agreement with the Cen A virial/orbital mass estimates and provides confirmation of the relatively high M/L_B of this elliptical-dominated group. The centroids of both the groups, as well as surrounding field galaxies, have very small peculiar velocities, $< 25 \text{ km s}^{-1}$, with respect to the local Hubble flow with $H_0 = 68 \text{ km s}^{-1} \text{ Mpc}^{-1}$.

Subject headings: galaxies: distances – galaxies galaxies: distances – galaxies galaxies: kinematics and dynamics

1. Introduction

The distribution of dark versus luminous matter on scales of 0.1 – 1.0 Mpc still remains poorly understood. The situation has been improving thanks to recent observations with Hubble Space Telescope (HST) that provide images of the resolved stellar content of hundreds of nearby galaxies. The brightness of the tip of the red giant branch (TRGB) in these images provide accurate distances. These accurate distances combined with accurate observed velocities, mostly from HI observations, allow for the decoupling of ‘peculiar’ velocities from the cosmic expansion. These peculiar velocities tell us something about the distribution of matter.

The observations of the nearest groups has been reviewed by Karachentsev (2005). Masses for the groups have been determined both by traditional measures of the internal group dynamics and by a method that uses the observed dimensions of groups at the radii of decoupling between group collapse and cosmic expansion. This location between collapse and expansion is called the “zero-velocity surface”. It has been found that for the 6 nearest groups the zero-velocity surface method gives mass-to-light ratios (B band) in the range [15 – 90] M_{\odot}/L_{\odot} with a median of 26 M_{\odot}/L_{\odot} . If these values were universal, they would imply a very low value for the density of matter, $\Omega_{m,local} \sim 0.04$. The observed “coldness” of the local Hubble flow, characterized by typical random motions $\sigma_v \sim 30$ km s⁻¹ (Karachentsev et al. 2002c), implies an extremely low value of Ω_m , unless modulated by the effects of vacuum-dominance (Chernin 2001).

Part of the discrepancy between very locally evaluated Ω_m and more global measures may be a consequence of large M/L variations with environment due to astrophysical processes like stellar aging and gas dispersal through heating (Tully 2005; van den Bosch et al. 2003). Although most of the light is in the “field”, a substantial fraction of the mass of the universe might be confined to dense clusters dominated by early-type galaxies. Consequently one must suitably average M/L over these distinct environments to arrive at estimates that are cosmologically meaningful. The local volume has a low density compared with clusters, such that in almost all the neighboring groups the dominant members are spiral galaxies. Bahcall et al. (2000) suggest that giant elliptical galaxies have more extended and ~ 3 times more massive halos than spiral ones.

We are learning about the nature of groups in our neighborhood. Karachentsev et al. (2002a, 2002b, 2003) have shown that the M 81/NGC 2403, Cen A/M 83, and Maffei 1/IC 342 groups are all “dumbbell” systems like the Local Group. In the best studied case beyond the Local Group, the M 81/NGC 2403 Group, the core around the foreground NGC 2403 sub-structure is clearly falling back toward the background M 81 sub-structure. Evidently, this group, like the Local Group, has semi-virialized cores and a larger bound, infalling zone. The masses inferred for the overall bound regions are essentially that of the sum of the cores.

The Cen A/M 83 region is particularly interesting because one of the dominant galaxies, Cen A, is a giant elliptical. The only other large elliptical nearby is the badly

obscured Maffei 1. With Cen A, we are offered the unique opportunity to study the outer halo of a giant elliptical in the same way we have been studying the environments of giant spirals. In a preliminary investigation (Karachentsev et al. 2002b) it was already seen that there are two distinct cores: around Cen A to the foreground and M 83 to the background. The two cores have the same radial velocities within the uncertainties of the observations so it is not clear if the two cores are bound or escaping from one another. Fortunately this region is rich in dwarf galaxies. These small galaxies provide test probes of the potential. Here, we present TRGB distances to galaxies in the wide vicinity of the nearby giant elliptical galaxy Cen A to flesh out the 3D view of the complex and improve our understanding of its dynamical state.

2. HST ACS photometry and Color–Magnitude diagrams

We have observed 24 galaxies with the Advanced Camera for Surveys (ACS) during HST Cycles 12 and 13 (proposals 9771 and 10235). We obtained 1200s F606W and 900s F814W images of each galaxy using ACS/WFC with exposures split to eliminate cosmic ray contamination. The cosmic ray cleaned images (CRJ data sets) were obtained from the STScI archive, having been processed according to the standard ACS pipeline.

Stellar photometry was obtained using the ACS module of DOLPHOT (Dolphin et al. in prep), using the recommended recipe and parameters. In brief, this involves the following steps. First, pixels that are flagged as bad or saturated in the data quality images were marked in the data images. Second, pixel area maps were applied to restore the correct count rates. Finally, the photometry was run. In order to be reported, a star had to be recovered with S/N of at least five in both filters, be relatively clean of bad pixels (such that the DOLPHOT flags are zero) in both filters, and pass our goodness of fit criteria ($\chi \leq 2.5$ and $|sharp| \leq 0.3$).

To estimate our photometric uncertainties and completeness, artificial star tests were run on the ESO 269-058 and KKs 55 fields, which represent the most and least crowded images. Completeness plots are shown in Figure 1. The plateau at $\sim 85\%$ completeness is due to bad pixels and cosmic rays. The magnitude errors as a function of recovered magnitude are shown in Figure 2. CTE corrections were made according to ACS ISR03-09, and our zero points and transformations were made according to Sirianni et al. (2005). We estimate the uncertainties in the calibration to be around 0.05 magnitudes.

We determined the TRGB using a Gaussian-smoothed I -band luminosity function for red stars with colors $V - I$ within $\pm 0^m.5$ of the mean $\langle V - I \rangle$ expected for red giant branch stars. Following Sakai et al. (1996), we applied a Sobel edge-detection filter. The position of the TRGB was identified with the peak in the filter response function. Uncertainty in measuring the TRGB was determined by performing bootstrap resampling. Drawing from the original luminosity function, every stellar magnitude has been displaced randomly following a gaussian distribution. Then a new luminosity function is determined and the

tip magnitude I_{TRGB} is calculated. This procedure was performed 1000 times for each galaxy. We take the standard deviation of the distribution of I_{TRGB} as the uncertainty. According to Da Costa & Armandroff (1990), the TRGB is located at $M_I = -4.05$ mag. The calibration relations were derived over the metallicity range of the Galactic globular clusters ($-2.1 \leq [Fe/H] \leq 0.7$) and are expected to work well over ages spanning 2 – 15 Gyr. Ferrarese et al. (2000) calibrated the zero point of the TRGB from galaxies with Cepheid distances and estimated $M_I = -4^m06 \pm 0^m07(random) \pm 0.13(systematic)$. A new TRGB calibration, $M_I = -4^m04 \pm 0^m12$, was made by Bellazzini et al.(2001) based on photometry and on a distance estimate from a detached eclipsing binary in the Galactic globular cluster ω Centauri. For this paper (as for our previous works with the HST data) we use $M_I = -4^m05$. We consider total errors in distance moduli to be the quadrature sum of the internal errors and external systematic errors. Internal errors include the uncertainties in the TRGB measurement, in the HST photometry zero point ($\sim 0^m05$), the aperture corrections ($\sim 0^m05$) and the uncertainties in extinction (A_I), which are taken to be 10% of the assumed values given by Schlegel et al. (1998). The external systematic error is the uncertainty in the $M_{I,TRGB}$ zero-point which is taken to be 0^m12 following Bellazzini et al.(2001).

3. TRGB distances and integrated properties of 24 galaxies

ACS images of 24 observed galaxies are shown in Figure 3. The compass in each field indicates the North and East directions. Usually our target galaxies were centered on the middle of the ACS field. In Figure 4 I versus $(V - I)$ color magnitude diagrams (CMDs) for the 24 galaxies are presented.

A summary of the resulting distance moduli for the observed galaxies is given in Table 1. Columns contain: (1) galaxy name, (2) equatorial coordinates, (3) radial velocity in km s^{-1} in the Local Group (LG) rest frame, (4) apparent I -band magnitude of the TRGB, and (second line) the uncertainty in measuring the TRGB, (5) the mean $V - I$ color measured at an absolute I magnitude -3.5 , correlated with metallicity (Lee et al. 1993), \pm rms uncertainty of the mean color, and (second line) the standard deviation of the RGB color, (6) Galactic extinction in the I -band from Schlegel et al. (1998), (7) true distance modulus in mag and total error in the distance modulus, (8) linear distance in Mpc, and (9) mean metallicity of the RGB with random and systematic errors divided by comma.

Some additional comments about the galaxy properties are briefly discussed below. The galaxies are listed in order by increasing Right Ascension.

ESO 215-09, KKs 40. This is an isolated dIrr galaxy of low surface brightness. It is noted in the Catalog of Neighboring Galaxies (Karachentsev et al. 2004 = CNG) as an object of very high hydrogen mass-to-luminosity ratio. Warren et al. (2004) performed surface photometry of the galaxy in B, V, R, I - bands and derived its HI line velocity field using ATCA. According to these data, the HI disk of ESO 215-09 extends over 6 Holmberg

radii, and the ratio of hydrogen mass to B -luminosity is $(22 \pm 4)M_{\odot}/L_{\odot}$.

ESO 381-20. HI mapping of this irregular galaxy was carried out by Côté et al. (2000). On our ACS frames the galaxy is resolved into more than 20 000 red and blue stars. Given its $M_{HI}/L_B = 2.6M_{\odot}/L_{\odot}$, ESO 381-20 has a considerable amount of gas and hence a strong potential to form new stars.

KK 182, Cen 6. This irregular galaxy of triangular shape was proposed as a member of the Cen A/M 83 complex by Côté et al.(1997) but it turns out to be slightly to the background.

ESO 269-058. This is a peculiar galaxy of I0 type with dusty patches. NED gives an erroneous velocity $+1853 \text{ km s}^{-1}$. It is seen in its CM diagram (Fig. 4) that the vast majority of $\sim 150\,000$ detected stars belong to the RGB population. The hydrogen mass-to-luminosity ratio, $0.07M_{\odot}/L_{\odot}$, turns out to be much lower than typical values for irregular galaxies.

KK 189. This dwarf spheroidal galaxy was not detected in the HI line by Huchtmeier et al. (2001). Jerjen et al. (2000b) did photometry of KK 189 in the B, R bands, deriving the total color of $B - R = 0.89$.

ESO 269-066, KK 190. This is a dSph galaxy undetected in HI (Huchtmeier et al. 2001). Its radial velocity, $+784 \text{ km s}^{-1}$, was measured via optical absorption lines by Jerjen et al. (2000a), who also carried out surface photometry of ESO 269-66 in B, R bands. The CM diagram of the galaxy derived by us (Fig. 4) displays a pronounced branch of red giant stars with a considerable metallicity scatter, unusual for galaxies of low luminosity (-13.6 mag).

KK 196, AM1318-444. Surprisingly, this dIrr galaxy is still undetected in HI. Its optical spectrum shows emission lines with the mean velocity $+741 \text{ km s}^{-1}$ (Jerjen et al. 2000b).

KK 197. This dSph galaxy, undetected in HI, is situated $48'$ away from NGC 5128 = Cen A. Its CM diagram (Fig. 4) displays a large scatter of colors for the stars near the tip of RGB. Our initial explanation of this atypical feature assumed the presence of a number of high metallicity stars projected from the periphery of Cen A onto the KK 197 field. However, the distribution of very red stars (situated to the right of the tip of RGB) shows a clear concentration within the boundary of KK 197. This implies that the observed scatter of colors (metallicities) of RGB stars is a property of the dwarf galaxy itself and not caused by outlying RGB stars in Cen A. Surface photometry of KK 197 in B, R bands was carried out by Jerjen et al. (2000b).

KKs 55. This dSph galaxy is the nearest known companion to Cen A at a distance of $39'$ in projection. CM diagram of KKs 55 exhibits that the vast majority of the detected stars belong to the RGB with small dispersion in their colors. The derived distance to KKs 55, 3.94 Mpc, coincides within errors with the distance to Cen A, 3.77 Mpc.

IC 4247, ESO 444-34. This is a dIrr galaxy of rather high surface brightness. Judging from the derived distance, 4.97 Mpc, IC 4247 is a companion to the bright spiral galaxy NGC 5236 = M 83.

NGC 5237. The compact reddish galaxy of I0 type has an irregular central part with an extended blue knot on the NW side and a smooth periphery. The CM diagram of NGC 5237 displays about 100 000 stars, mainly belonging to the RGB. The blue stellar population of the galaxy is concentrated towards its core.

KKs 57. This galaxy of very low surface brightness is classified as type dSph or dSph/Ir. It is not detected in the HI line by Huchtmeier et al. (2001). KKs 57 is one of the faintest known companions to Cen A with $M_B = -10.3$ mag.

HIPASS1348-37. This is a dIrr galaxy found in the blind HI survey of the southern sky with the Parkes Telescope (Banks et al. 1999). The coordinates presented in NED are rather inaccurate.

ESO 383-87. In our list, this bright ($B = 11.0$ mag) spiral galaxy of SBdm type has the lowest radial velocity, $V_{LG} = +108$ km s⁻¹. Amazingly, it was never resolved into stars before. Kemp & Meaburn (1994) noted that the galaxy is embedded in an extensive fairly spherical halo seen down to the level of 2% of the sky brightness. Unfortunately, ESO 383-87 was imaged with ACS in the F814W filter only, because of an HST guiding problem. Another F814W image of the galaxy has been obtained with WFPC2 (GO #8599). We carried out photometry of both the images and obtained an *I*-band luminosity function of ESO 383-87. Applying the edge-detection Sobel filter to the luminosity function, we derived the TRGB positions 23.76 (WFPC2) and 23.78 mag (ACS), which yields the galaxy distance to be 3.45 ± 0.34 Mpc. It is by far preferable to have the color information provided by a *V* filter observation but in this case the onset of the red giant branch is sufficiently distinct that the distance measure based on the *I* observation alone is considered reliable. Basing on the measured TRGB distance, we assign the galaxy to be a companion to Cen A.

HIPASS1351-47. This dIrr galaxy of low surface brightness was found in the HIPASS survey (Banks et al. 1999). Its coordinates given in NED differ from true ones by 2'.5. The large TRGB distance to the galaxy together with its low radial velocity, $V_{LG} = 292$ km s⁻¹, indicates that the galaxy is located behind the Cen A/M 83 complex and has a noticeable peculiar velocity towards the complex.

ESO 384-016. This is a galaxy of dS0/Im type with a diffuse halo around a compact central core. Jerjen et al. (2000a,b) performed surface photometry of the galaxy in *B*, *R* bands and estimated its distance via surface brightness fluctuations to be 4.23 Mpc. Our estimate of the galaxy distance from the TRGB, 4.53 Mpc, is in good agreement.

ESO 223-09. This isolated dIrr galaxy is situated behind and East of the Cen A/M 83 complex in a zone of strong extinction. The galaxy has a lot of gas ($2.2M_{\odot}/L_{\odot}$) for continuing star formation. It is seen in the CMD of Fig. 4 that this galaxy has a pronounced

intermediate age asymptotic giant branch population. These stars lie immediately above the red giant branch but the onset of the RGB is sufficiently dominant that the TRGB can be clearly distinguished.

ESO 274-01, RFGC 2937. This is an isolated Sd galaxy seen edge-on. With its angular dimension of $13'.4 \times 1'.3$, only a small part of the galaxy is situated within the ACS field of view. Nevertheless, our photometry reveals more than 100,000 stars, the majority belonging to the RGB. The measured TRGB distance, 3.09 Mpc, together with the galaxy radial velocity, $V_{LG} = +335 \text{ km s}^{-1}$, may indicate a peculiar motion of ESO 274-01 away from us toward the Cen A/M 83 complex.

ESO 137-18. This is an isolated galaxy of type Sm or Im in the zone of the Milky Way ($b = -7.^\circ 4$). In spite of significant contamination by foreground stars, its CM diagram displays the RGB population, yielding the galaxy distance of 6.40 Mpc. As with ESO 223-09, there is a substantial intermediate age population that gives rise to a well populated asymptotic giant branch. Nonetheless the TRGB is easily identified.

Apart from the galaxies discussed above, we also observed the galaxy PGC 47885 reported to have a radial velocity of $+570 \text{ km s}^{-1}$. This object turns out to be a distant spiral galaxy unresolved into stars. According to recent 6dF data (see NED), its radial velocity is $+13848 \text{ km s}^{-1}$.

4. The turn-over radius of the Cen A/M 83 complex

The list of all known galaxies in a wide vicinity within a radius of ~ 4 Mpc around the centroid of the complex Cen A/M 83 is presented in Table 2. The list contains 87 galaxies. Some galaxies (for instance, DDO 161) have radial velocities $V_{LG} < 550 \text{ km s}^{-1}$, but they have no individual distance estimates. For other galaxies (for instance, the dwarf spheroidal system KK 197) the distances are measured with high accuracy, but the radial velocities are lacking. The columns of Table 2 contain the following data: (1) galaxy name; (2) equatorial coordinates for the epoch J2000; (3) morphological type; (4) “tidal index” following from the Catalog of Neighboring Galaxies (Karachentsev et al 2004 :CNG): for every galaxy “ i ” we found its “main disturber” (=MD), producing the highest tidal action

$$\Theta_i = \max\{\log(M_k/D_{ik}^3)\} + C, \quad (i = 1, 2 \dots N)$$

where M_k is the total mass of any neighboring potential MD galaxy (proportional to its luminosity with $M/L_B = 10M_\odot/L_\odot$) separated from the considered galaxy by a space distance D_{ik} ; the value of the constant C is chosen so that $\Theta = 0$ when the Keplerian cyclic period of the galaxy with respect to its MD equals the cosmic Hubble time, $1/H_0$; therefore positive values correspond to galaxies in groups, while the negative ones correspond to isolated galaxies; (5) radial velocity of the galaxy with respect to the Local Group centroid and its error; (6) distance to the galaxy (in Mpc) and its error; (7) method of estimating the distance (“cep” — from cepheids, “rgb” — from the tip of RGB, “sbf” — from surface

brightness fluctuations, “mem” — from probable membership in the known groups, “h” — from radial velocity with the global Hubble constant $H_0 = 72 \text{ km s}^{-1}\text{Mpc}^{-1}$, Freedman et al. 2001); (8) reference to the source of data on the distance or a new radial velocity; and (9) notes regarding galaxy membership in the Cen A (“C”) and M 83 (“M”) groups based on a positive tidal index with respect to Cen A or M 83.

The greater part of the data on galaxy distances are taken from the CNG although more than 40% of estimates have appeared over the last two years. Apart from 24 new distance measurements from Table 1 (=K06b), we have used distance estimates of galaxies based on TRGB measurements by Tully et al. (2006)= T06, Karachentsev et al. (2006a)= K06a, Rejkuba (2004)=R04, bf Sakai et al. (2004), Galazutdinova (2005) = G05, and Sharina (2005)= Sh05. New radial velocities for 5 galaxies from the HIPASS survey were taken from Koribalski et al. 2004 (=Ko04) and Meyer et al. 2004 (=M04). For two dSph galaxies, KK 211 and KK 221, new optical radial velocities were recently measured by Puzia & Sharina (2006) via globular clusters. For the spiral galaxy Circinus situated in the Zone of Avoidance, we have determined its distance modulus from the Tully-Fisher relationship in the J , H and K bands based on the data of the 2MASS survey. There is another probable member of the Cen A group, ESO 270-17 = RFGC 2603. This large (15′ diameter) SBm type galaxy seen edge-on has $V_{LG} = 583 \text{ km s}^{-1}$, a bit exceeding our velocity cutoff. We have derived its TF distance modulus based on B, R, I magnitudes to be 28.18 ± 0.37 that comfortably puts ESO 270-17 in the Cen A suite.

Because of its luminosity and probable dynamic importance, we give special attention to the giant spiral galaxy NGC 5236 = M 83. In the CNG it was listed with the cepheid distance $4.47 \pm 0.30 \text{ Mpc}$ (Thim et al. 2003), which positions M 83 to the foreground of all its companions with TRGB distances. We ran DOLPHOT photometry on archival ACS images of the M83 halo (program 9864), The resulting CMD is shown in Fig. 5. There is some uncertainty because of the spread of stellar metallicity but the cepheid distance seems underestimated. Applying the edge-detection Sobel filter, we derived the TRGB position to be $I(\text{TRGB}) = 24.64 \pm 0.15$ within a color range of $1.0 < (V - I) < 2.0$, which yields the galaxy distance $5.16 \pm 0.41 \text{ Mpc}$. On the northern edge of M 83 there is a faint elongated arc, KK 208, a possible satellite dSph galaxy disrupted by M 83’s tidal forces. Its TRGB distance, $4.68 \pm 0.47 \text{ Mpc}$, is at middle of the M83 cepheid and TRGB distances.

The overall distribution on the sky of the galaxies from Table 2 is presented in Fig. 6. The galaxies with individual distance estimates are shown by circles, while the galaxies with distances obtained from the Hubble relation are marked by squares. To attach an impression of depth to this distribution, the galaxy radial velocities are given colors following the scale on the right side of the figure.

A 3-dimensional view of the Cen A/M 83 complex and its surroundings is presented in Fig. 7 where brighter galaxies are shown as larger balls. Spiral – irregular galaxies, and elliptical – dwarf spheroidal galaxies with accurate (“cep” and “rgb”) distances are drawn as blue and red balls, respectively.

The Hubble diagram for galaxies in the Cen A/M 83 complex and its closest surrounding is shown in Fig. 8. Galaxies in groups and in the general field are depicted by open and filled circles, respectively. Galaxies for which Cen A and M 83 are main attractors are joined with these dominant systems by solid lines. Both the radial velocities and the distances are given in relation to the Local Group centroid. The two dashed lines correspond to alternate choices of the Hubble parameter, the global value of $72 \text{ km s}^{-1} \text{ Mpc}^{-1}$, (Freedman et al. 2001) and the mean local value $68 \text{ km s}^{-1} \text{ Mpc}^{-1}$, (Karachentsev et al. 2006), curved because of the decelerating action of the Local Group with a total mass of $1.3 \cdot 10^{12} M_{\odot}$.

As we had come to anticipate, field galaxies show a markedly lower peculiar velocity dispersion than that of the members of the groups. Field galaxies are also seen to have a tendency to move toward the Cen A/M 83 complex. This motion is manifested as the known wave effect around an attractor: galaxies on the near side of the complex have velocities higher than the Hubble expectation and galaxies on the far side have velocities lower than the Hubble expectation. The distances and velocities of the main galaxies, Cen A and M 83, coincide within errors with the mean distance and the mean velocity of their companions. That is, Cen A and M 83 are not only the centers of both groups according to their position in the sky, but also the dynamical centers of these groups. Here, the peculiar velocities of the group centroids with respect to the mean local Hubble flow at $H_0 = 68 \text{ km s}^{-1} \text{ Mpc}^{-1}$ do not exceed 25 km s^{-1} .

A rough estimate of the radius of the zero-velocity sphere, R_0 , can be made considering the mutual motion of the main members of the groups, Cen A and M 83. The spatial separation between them is $R_{gg} = (1.73 \pm 0.56) \text{ Mpc}$. Assuming that their mutual tangential motion is zero, the difference of their radial velocities projected onto the line joining the galaxies is equal to $(V_{M83} - V_{CenA}) = +35 \pm 6 \text{ km s}^{-1}$. It would take a tangential motion of 69 km s^{-1} of the two galaxies toward each other for one to see the other at zero velocity. If the galaxies M 83 and Cen A are receding from each other, as is suggested but not certain, then R_0 is less than R_{gg} . Alternatively, consider the motions of the group centroids. We obtained from Table 2 the mean values $\langle V \rangle = 292 \pm 37 \text{ km s}^{-1}$ and $\langle D \rangle = 3.76 \pm 0.05 \text{ Mpc}$ for the Cen A group, and $\langle V \rangle = 318 \pm 22 \text{ km s}^{-1}$ and $\langle D \rangle = 4.79 \pm 0.10 \text{ Mpc}$ for the M 83 group. Under the same assumption that the relative tangential motions of the groups are zero, we obtain that the centers of groups are moving apart from one another at a velocity of $+70 \pm 30 \text{ km s}^{-1}$ at a mutual spatial separation $R_{cc} = (1.43 \pm 0.11) \text{ Mpc}$.

A more detailed approach to determining the radius R_0 was used by Karachentsev & Kashibadze (2006). They considered the velocity field around the Local Group of galaxies with accurate distance estimates and obtained the value $R_0(LG) = 0.96 \pm 0.03 \text{ Mpc}$. By varying the mass center between the two main members of the LG and seeking a minimum scatter of galaxies on the Hubble diagram, Karachentsev & Kashibadze (2006) estimated a mass ratio of 0.8:1.0 for our Galaxy and M 31, in accordance with the observed ratio of luminosities of these galaxies. A similar analysis of the velocity field of the galaxies around the M 81 group yielded the value of $R_0(M81) = 0.89 \pm 0.05 \text{ Mpc}$ and the ratio of masses

of two main galaxies, M 81 and M 82, of 1.0:0.5, in good agreement with the ratio of the luminosities of these galaxies.

Examining the Hubble pattern around the complex Cen A/M 83, we suppose the center of mass of the complex to be coincident with Cen A, then we determine velocities V and distances R of the galaxies given in Table 2 with respect to Cen A. Here, we take into account only the objects whose separations from Cen A along the line of sight exceed their projected separations on the sky: $|D_g - D_c| > R_p$, and also excluded close companions ($R < 1$ Mpc) in order to reduce the contribution from virial motions. At total, there are 18 galaxies with spatial distances from Cen A, $1 < R < 4$ Mpc which are comfortably situated along a line of sight passing through Cen A. Surprisingly, all of them reside behind the Cen A group. The resulting Hubble diagram for them is presented in Fig. 9. Each galaxy is shown by a circle with horizontal and vertical bars denoting standard errors of distance and velocity. Galaxies in groups ($\Theta > 0$) and in the general field ($\Theta < 0$) are indicated by open and filled circles, respectively. The solid line in Fig. 9 corresponds to the Hubble regression with $H_0 = 72 \text{ km s}^{-1} \text{ Mpc}^{-1}$ and the R_0 value which ensures the minimum scatter of galaxies with respect to the Hubble regression. As is seen, the regression line crosses the zero-velocity line at $R_0 = 1.40 \pm 0.11$ Mpc, where the standard deviation, 0.11 Mpc, is a bootstrap estimate. The mean-square peculiar velocity of the galaxies relative to the homogeneous Hubble flow is 32 km s^{-1} . However, this value is affected to a considerable degree by measurement errors in galaxy distances. After quadratic subtraction of observational errors, the typical peculiar velocity drops to 2 km s^{-1} .

Thus, the Hubble flow around the Cen A/M 83 complex proves to be rather cold. Low velocities of chaotic motions $\sim (10 - 20) \text{ km s}^{-1}$ are characteristic also of the surroundings of two other nearby complexes: the Local Group and the M 81 group. This feature is direct evidence of the existence of dark energy which dominates at distances $\gtrsim 1$ Mpc from the center of a typical loose group of galaxies.

5. Mass estimates of the complex Cen A/M 83

The separation of galaxies in the Centaurus region into the Cen A and M 83 groups was considered in detail by Karachentsev et al. (2002b). They measured masses for the two groups from the virial theorem

$$M_{vir} = 3\pi N \times (N - 1)^{-1} \times G^{-1} \times \sigma_v^2 \times R_H,$$

where σ_v^2 is the dispersion of radial velocities with respect to the group centroid, and R_H is the mean projected harmonic radius, or from the orbital motions of companions around the principal galaxy,

$$M_{orb} = (32/3\pi) \times G^{-1} \times (1 - 2e^2/3)^{-1} \langle R_p \times \Delta V_r^2 \rangle,$$

assuming arbitrarily oriented Keplerian orbits of companions with the mean eccentricity of galaxy orbits postulated to be $e = 0.7$. New observational data modifies the mass estimates.

Basing on radial velocities and mutual separations of supposed members of Cen A group (marked in the last column of Table 2 as “C”), we obtained the mean harmonic radius of the group $R_H = 192$ kpc and the radial velocity dispersion $\sigma_v = 136$ km s⁻¹, which yields a virial mass of the group $M_{vir} = 8.1 \cdot 10^{12} M_\odot$. The orbital mass estimate turns out to be somewhat smaller, $M_{orb} = 6.4 \cdot 10^{12} M_\odot$.

The new values of the harmonic radius and radial velocity dispersion for the M 83 group are 89 kpc and 61 km s⁻¹, respectively. Mass estimates for the M 83 group, $M_{vir} = 0.82 \cdot 10^{12} M_\odot$ and $M_{orb} = 0.89 \cdot 10^{12} M_\odot$, are almost an order of magnitude lower than for the Cen A group.

The total blue luminosities of these groups, $L_B(\text{CenA}) = 6.0 \cdot 10^{10} L_\odot$ and $L_B(\text{M 83}) = 2.5 \cdot 10^{10} L_\odot$, differ from one another much less than the mass estimates. This situation is consistent with the proposition (Bahcall et al. 2000; Tully 2005) that giant elliptical galaxies, as well as groups with a predominantly elliptical population, have masses per unit luminosity about 3 times higher than giant spirals or groups with predominantly spiral populations. In the present case, the elliptical dominated Cen A group has a mass-to-light ratio $M/L_B = 125 M_\odot/L_\odot$ while the spiral dominated M 83 group has $M/L_B = 34 M_\odot/L_\odot$. This difference cannot be attributed only to the presence in spiral galaxies of a young (blue) stellar population and dust clouds since the infrared luminosities in the K - band, $L_K(\text{CenA}) = 15.1 \cdot 10^{10} L_\odot$ and $L_K(\text{M 83}) = 7.1 \cdot 10^{10} L_\odot$, taken from 2MASS, also differ far less than the mass estimates of the groups.

Consideration of galaxy motions in the vicinity of the Cen A/M83 complex gives us a mass estimate on a scale of ~ 1 Mpc. According to Lynden-Bell (1981) and Sandage (1986), the total mass of a group is expressed via the turn-over radius R_0 and the age of the universe T_0 as

$$M_T = (\pi^2/8G) \cdot R_0^3 \cdot T_0^{-2}. \quad (1)$$

where G is the gravitation constant. In the “concordant” flat cosmological model with a non-zero Λ - term, equation (1) needs to be modified as

$$M_T = (\pi^2/8G) \cdot R_0^3 \cdot H_0^2 \cdot f(\Omega_m)^{-2}, \quad (2)$$

where

$$f(\Omega_m) = 1/(1 - \Omega_m) - 0.5 \cdot \Omega_m \cdot (1 - \Omega_m)^{-1.5} \cdot \text{arccosh}[(2/\Omega_m) - 1] \quad (3)$$

For $\Omega_m = 0.27$, we have $f(0.27) = 0.82$, and with $H_0 = 72$ km s⁻¹ Mpc⁻¹ corresponding to $T_0 = 13.7$ Gyr, we obtain a new expression for the total mass: $(M_T/M_\odot) = 2.2 \cdot 10^{12} (R_0/\text{Mpc})^3$, yielding $M_T = (6.0 \pm 1.4) \cdot 10^{12} M_\odot$. Thus, the mass estimates of the Cen A group made from galaxy motions internal and external to the group are in good agreement at $6 - 8 \cdot 10^{12} M_\odot$.

The outer halo of Cen A has been recently studied by Peng et al. (2004) based on the kinematics of 148 planetary nebulae situated at radii beyond 20 kpc. Applying different dynamical models, they obtained the total mass of the galaxy within 80 kpc to be $(5.0 - 5.9) \cdot 10^{11} M_\odot$. This mass is much lower than our estimates presented above. Part

of the difference is due to the factor 5 difference in scale. Another factor of 2–3 remains unexplained. By contrast, we have good agreement with the dynamical study of globular clusters around Cen A by Woodley (2006). The motions of 340 globular clusters within a radius of 45 kpc imply a mass of $(0.8 - 1.8) \cdot 10^{12} M_{\odot}$. We find a mass 6 times greater on a scale 9 times greater.

We can make a comparison with a statistical measure of group masses. Over the last years, a new possibility of determining the total mass of groups has appeared based on measuring a signal of weak lensing of more distant galaxies. Hoekstra et al. (2005) detected such a signal by measuring the orientation of the major axes of background galaxies around single “lens galaxies” with photometric redshifts $z = 0.2 - 0.4$. The giant galaxies Cen A and M 83 would look at these distances like ordinary field galaxies. From the data by Hoekstra et al. (2005), galaxies like Cen A and M 83 with their blue luminosities 3.1 and $2.3 \cdot 10^{10} L_{\odot}$ generate a signal of lensing on a scale of ~ 0.5 Mpc which corresponds to a total mass of $(3.8 \pm 1.4) \cdot 10^{12} M_{\odot}$. This estimate of mass is quite consistent with our estimate of the total mass of Cen A/M 83 made from the distortion to the Hubble velocity field around the Cen A/M 83 complex.

6. Concluding remarks

We have presented new distances to 24 galaxies situated in the nearby binary group Cen A/M 83 and its vicinity. A total of 87 galaxies are presently known inside a sphere of radius ~ 4 Mpc around the centroid of the complex. Among them, 17 dwarf spheroidal galaxies do not yet have measured radial velocities. Among 66 galaxies with individual distance estimates, for 2 galaxies the distances were measured via the luminosity of cepheids, for 61 galaxies the distances were determined by the TRGB method, and for 3 galaxies the distances were estimated from the Tully-Fisher relation or surface brightness fluctuations. Thus, another 21 galaxies in the volume under discussion are targets for future distance measurements.

Considering galaxies only in close proximity to Cen A and M 83, we determined the total (virial or orbital) mass of the whole Cen A/M 83 complex to be $(6.4 - 8.1) \cdot 10^{12} M_{\odot}$ with 90% of the mass associated with the component around Cen A. An independent estimate of the mass of the Cen A component was made from the distortion of the cosmic expansion velocity field among the galaxies surrounding the complex. The observed deceleration of neighboring galaxies caused by the mass of the Cen A group is characterized by the sphere of radius R_0 which separates the group from the general cosmological expansion. The radius R_0 about Cen A lies in the range 1.29 – 1.51 Mpc, which corresponds to a mass $(6.0 \pm 1.4) \cdot 10^{12} M_{\odot}$ in a model with $\Omega_{\Lambda} = 0.73$, $\Omega_m = 0.27$. This mass estimate is in excellent agreement with the mass estimates from the internal motions in the Cen A group.

Estimates of the total mass of Cen A are listed in Table 3. Ordered by scale length,

they probe the scale range from 80 to 1400 kpc. Apart from the first mass estimate (PNe dynamics), the remaining ones agree with each other within $2\text{-}\sigma$ significance levels. This agreement is satisfactory because every method is subject to substantial uncertainties.

The key result of our observations is the determination of $M/L_B = 125 M_\odot/L_\odot$ for the Cen A group. In the cases of nearby groups dominated by the giant spirals M31, M81, and M83, the identical methods of calculating masses results in estimates of M/L_B of 16, 32, and 34, respectively. This evidence supports the proposition that environments that have dynamically evolved to the end-state of elliptical galaxies have dark matter halos that manifest less light than the less evolved environments of spirals.

Support associated with HST programs 9771 and 10235 was provided by NASA through a grant from the Space Telescope Science Institute, which is operated by the Association of Universities for Research in Astronomy, Inc., under NASA contract NAS5-26555. This work was also supported by RFFI grant 04-02-16115. This study has made use of the NASA/IPAC Extragalactic Database (NED), the HI Parkes All Sky Survey (HIPASS), and the Two Micron All-Sky Survey.

REFERENCES

- Bahcall N.A., Cen R., Davé R. et al. 2000, ApJ 541, 1
- Banks G.D., Disney M.J., Knezek P.M., et al., 1999, ApJ 524, 612
- Bellazzini M., Ferraro F.R., Pancino E., 2001, ApJ 556, 635
- Chernin A.D., 2001, Physics-Uspekhi 44, 1099
- Côté S., Freeman K.C., Carignan C., Quinn P.J., 1997, AJ 114, 1313
- Côté S., Mateo M., Sargent W.L.W., Olszewski E.W., 2000, ApJ 537, L91
- Da Costa G.S., Armandroff T.E., 1990, AJ 100, 162
- Ferrarese L., et al. 2000, ApJ 529, 745
- Freedman W.L., et al. 2001, ApJ, 553, 47
- Galazutdinova O.A., 2006, personal communication
- Hoekstra H., Hsieh B.C., Yee H.K., Lin H., Gladders M.D., 2005, ApJ, 635, 73
- Huchtmeier W.K., Karachentsev I.D., Karachentseva V.E., 2001, A&A 377, 801
- Jerjen H., Binggeli B., Freeman K.C., 2000b, AJ 119, 593
- Jerjen H., Freeman K.C., Binggeli B., 2000a, AJ 119, 166
- Karachentsev I.D., 2005, AJ 129, 178
- Karachentsev I.D., Dolphin A.E., Geisler D., et al. 2002a, A&A 383, 125
- Karachentsev I.D., Dolphin A., Tully R.B., et al. 2006, AJ, 131, 1361
- Karachentsev I.D., Karachentseva V.E., Huchtmeier W.K., Makarov D.I., 2004, AJ 127, 2031
- Karachentsev I.D., Kashibadze O.G., 2006, Astrofizika 49, 5
- Karachentsev I.D., Sharina M.E., Dolphin A.E., et al. 2002b, A&A 385, 21
- Karachentsev I.D., Sharina M.E., Makarov D.I., et al. 2002c, A&A 389, 812
- Karachentsev I.D., Sharina M.E., Dolphin A.E., Grebel E.K., 2003, A&A 408, 111
- Kemp S.N., Meaburn J., 1994, A&A 289, 39
- Koribalski B.S., Stavely-Smith L., Kilborn V.A. et al. 2004, AJ, 128, 16

- Lee, M. G., Freedman, W. L., Madore, B. F., 1993, ApJ 417, 553
- Lynden-Bell D., 1981, Observatory 101, 111
- Meyer M.J., Zwaan M.A., Webster R.L., et al. 2004, MNRAS, 350, 1195
- Peng E.W., Ford H.C., Freeman K.C., 2004, ApJ, 602, 685
- Puzia T.H., Sharina M.E., 2006, personal communication
- Rejkuba M., 2004, A&A 413, 903
- Sakai S., Ferrarese L., Kennicutt R., Saha A., 2004, 608, 42
- Sakai S., Madore B.F., Freedman W.L., 1996, ApJ 461, 713
- Sandage A.R., 1986, ApJ 307, 1
- Schlegel, D.J., Finkbeiner, D.P., & Davis, M., 1998, ApJ 500, 525
- Sharina M.E., 2005, personal communication
- Sirianni M., Jee M.J., Benitez N. et al., 2005, PASP (in press)
- Spergel D.N., Verde L., Peiris H.V. et al. 2003, ApJS 148, 175
- Thim F. et al. 2003, ApJ, 590, 256
- Tully R.B., 2005, ApJ 618, 214
- Tully R.B., Rizzi, L., Dolphin, A.E., et al. 2006, AJ, 132, 729
- van den Bosch, F.C., Yang, X., Mo, H.J. 2003, MNRAS 340, 771
- Warren B.E., Jerjen H., Koribalski B.S., 2004, AJ 128, 1152
- Woodley, K., 2006, astro-ph/0608497

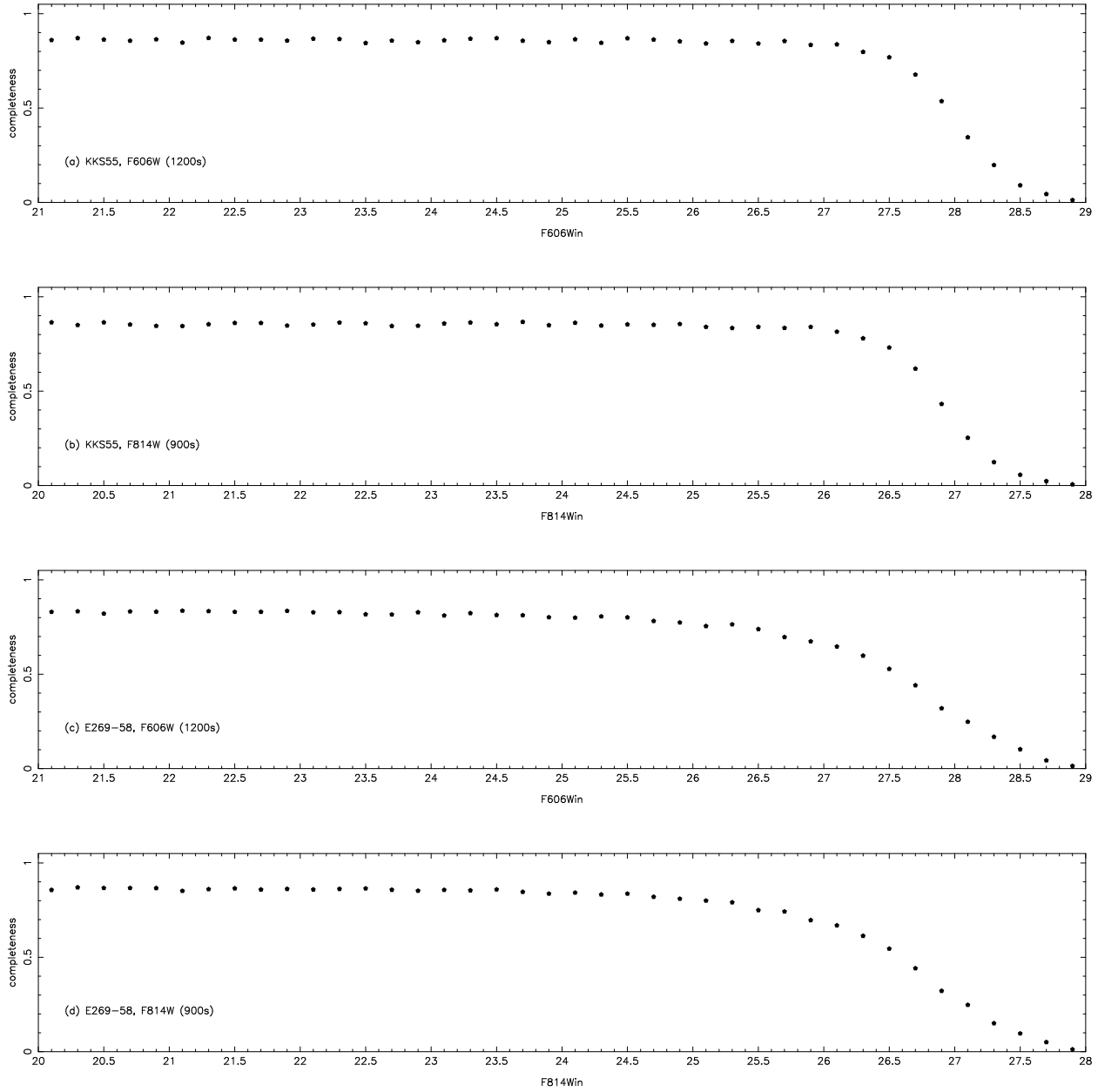


Fig. 1.— Photometric completeness as a function of magnitude for the least crowded (KKs 55) and the most crowded (ESO 269–58) galaxies.

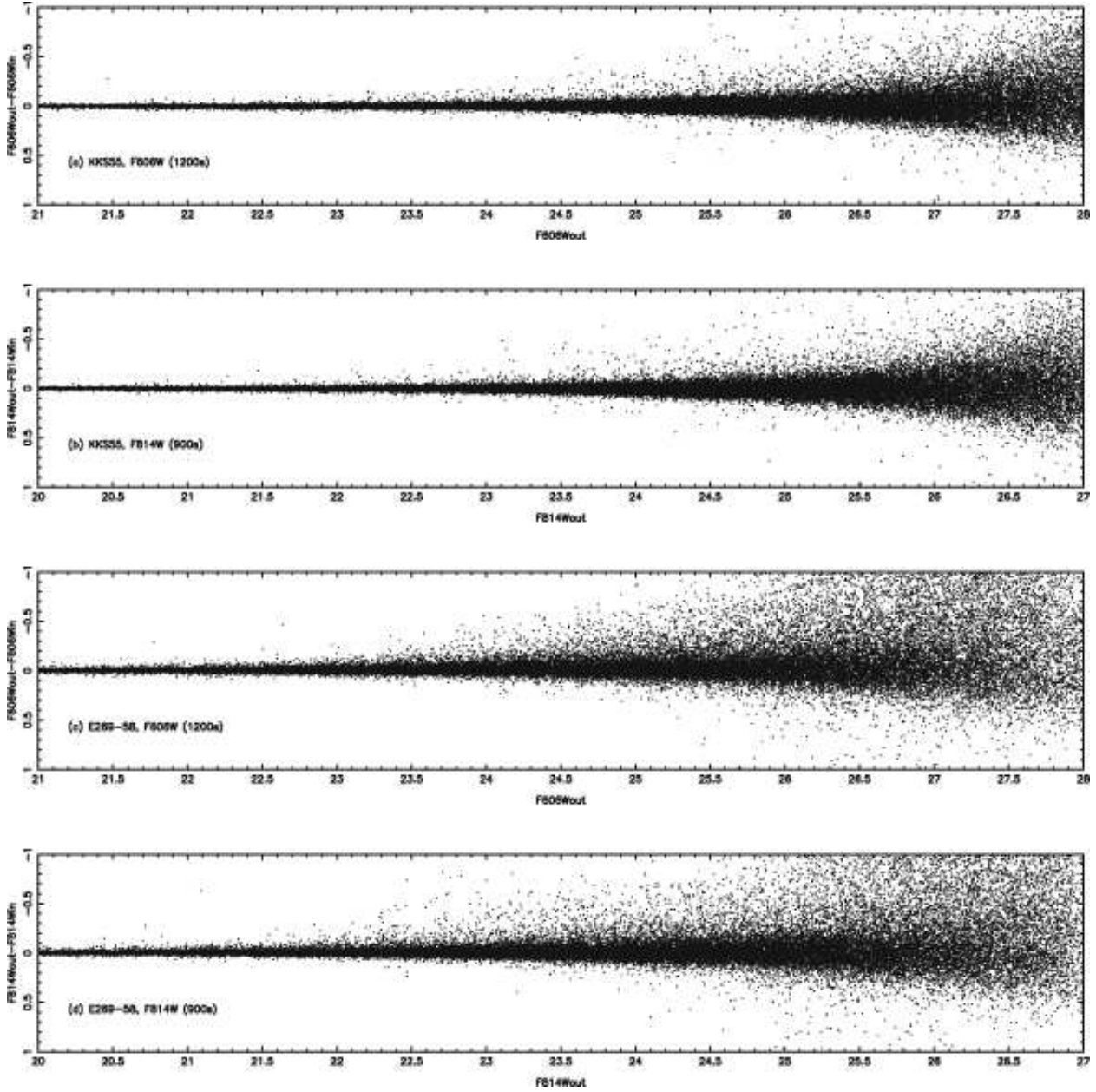


Fig. 2.— Mean photometric error as a function of magnitude for KKs 55 and ESO 269–58.

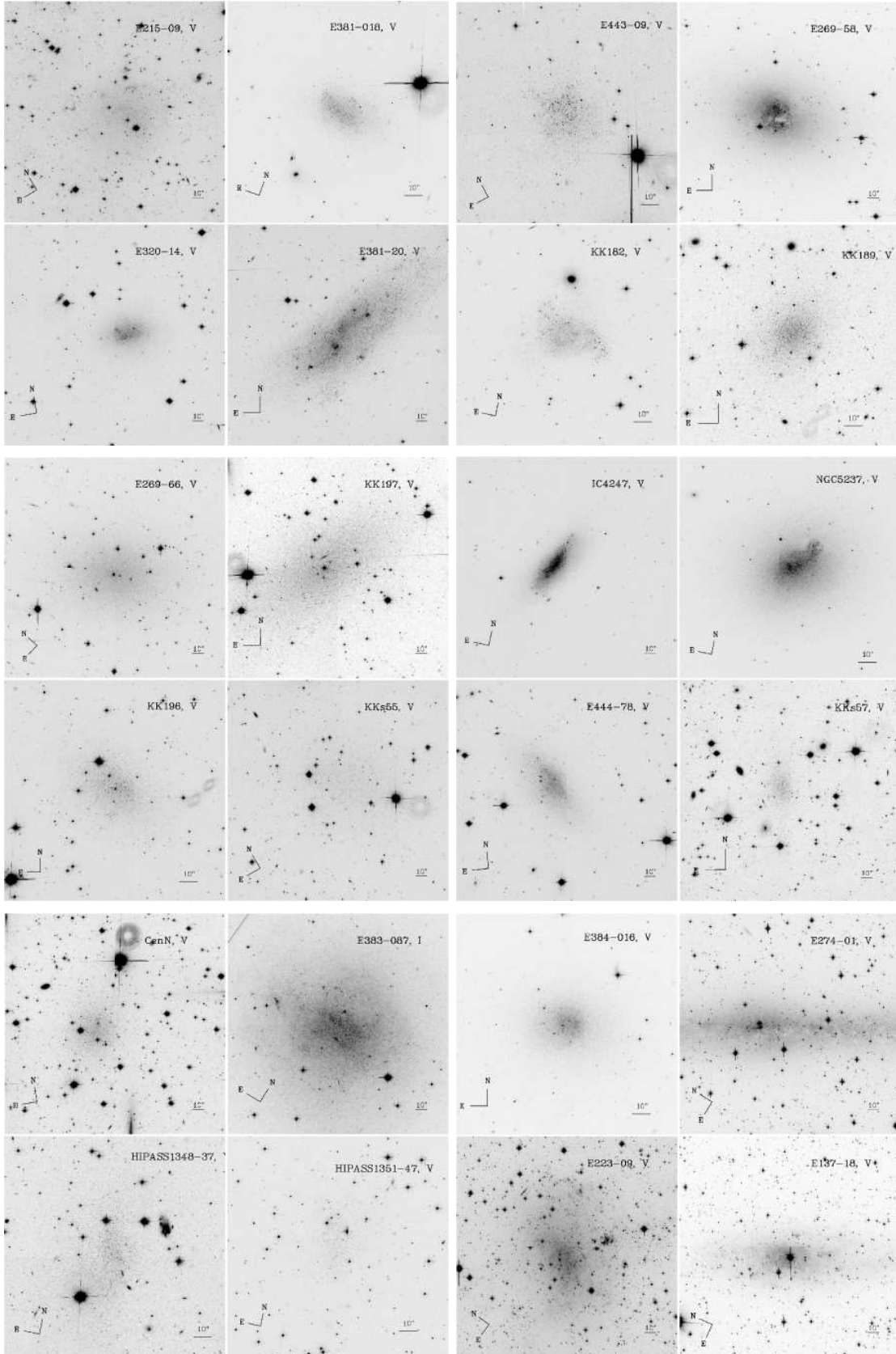


Fig. 3.— ACS “V” images of 24 nearby galaxies; 23 from two 600 second exposures in F606W and one (ESO 383-87) from two 450 second exposures in F814W.

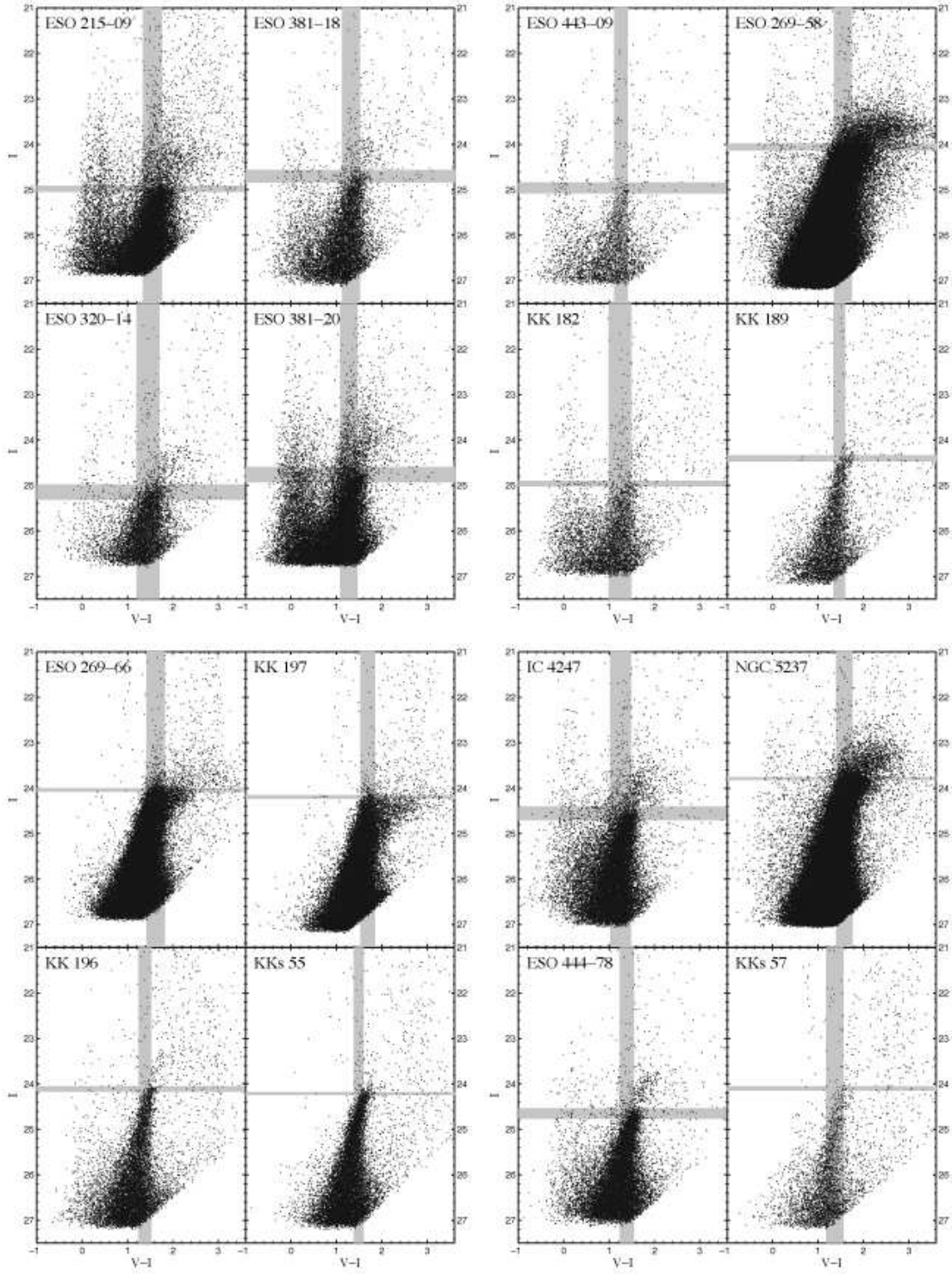


Fig. 4.— ACS color-magnitude diagrams for 23 nearby galaxies in the Cen A/M 83 area. The uncertainties in the TRGB measurement and in the RGB mean color $\langle V - I \rangle_{-3.5}$ are shown as shaded regions.

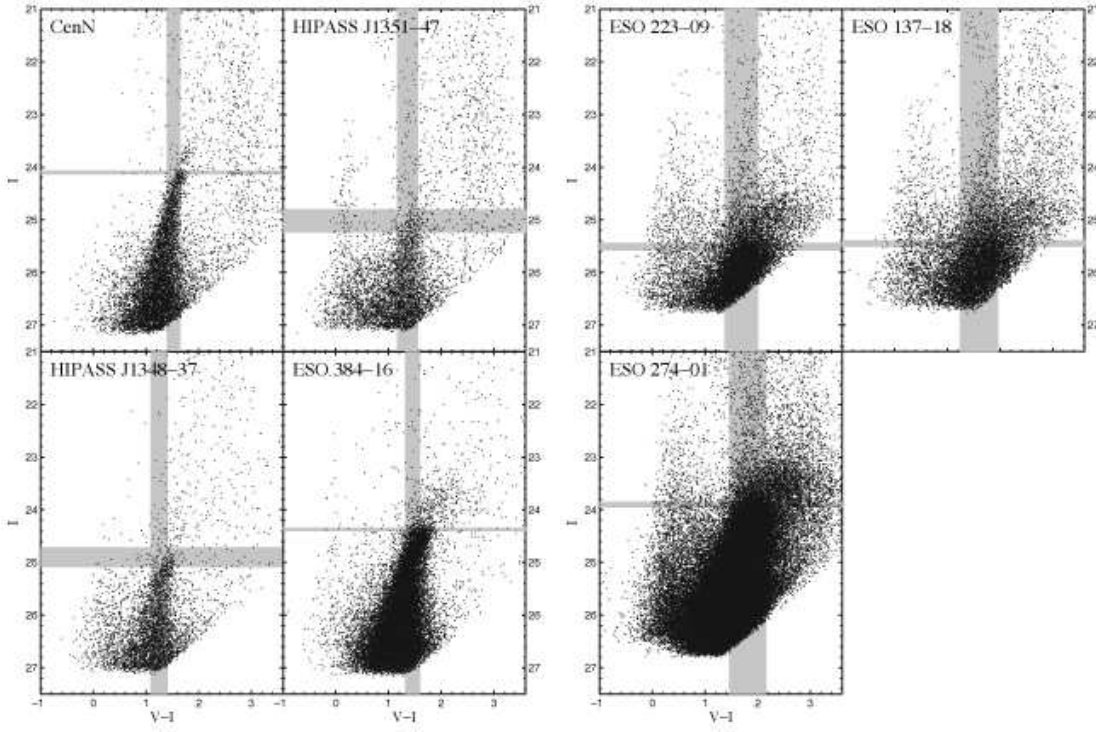


Fig. 4.— continued

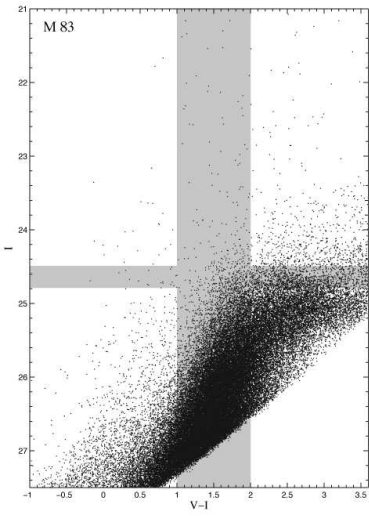


Fig. 5.— ACS color-magnitude diagram for M83. The color measurement range and TRGB magnitude uncertainty range are shown as shaded regions.

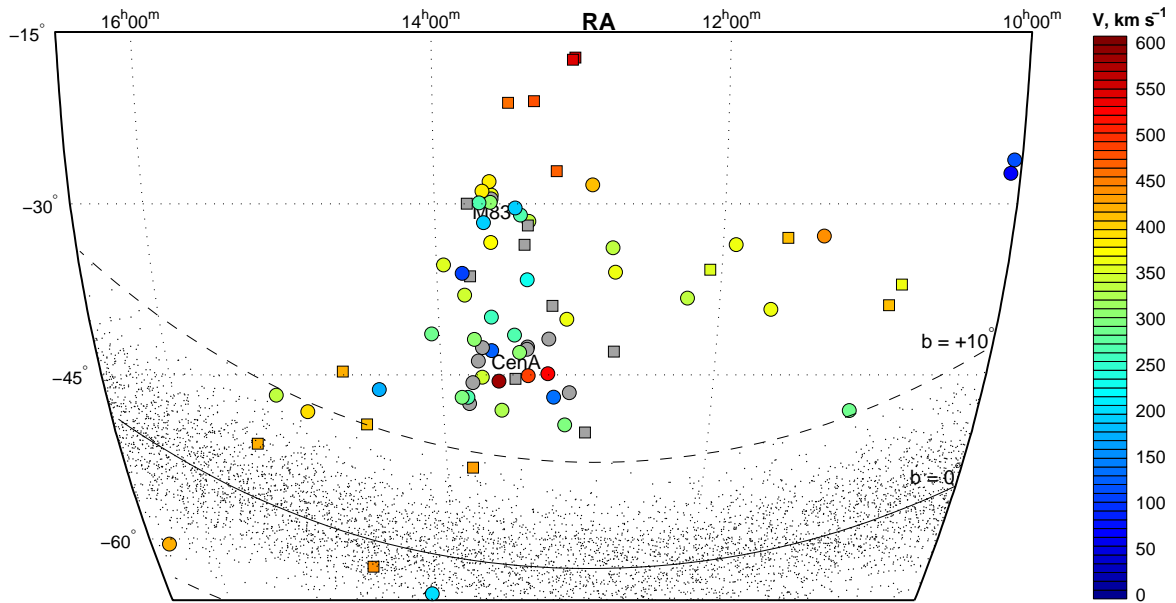


Fig. 6.— The distribution of galaxies in and around the Cen A/M 83 complex. The galaxies with individual distance estimates are shown by circles, while the galaxies with distances obtained from the Hubble relation are marked by squares. Radial velocities of galaxies are indicated by different colors. The Milky Way zone of avoidance is shown as the dotted area.

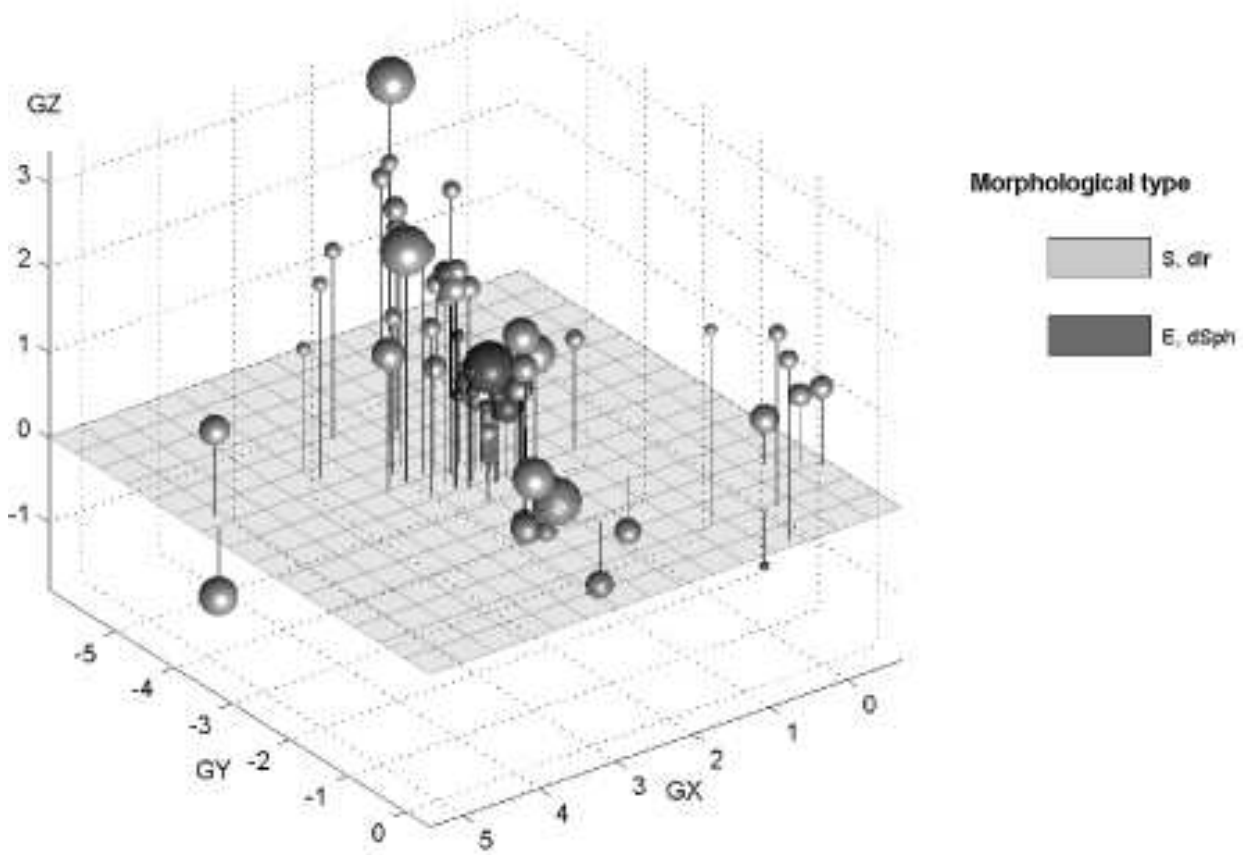


Fig. 7.— The 3D- view of the Cen A/M 83 complex. Galaxies of young and old stellar population are shown by light and dark grey, respectively.

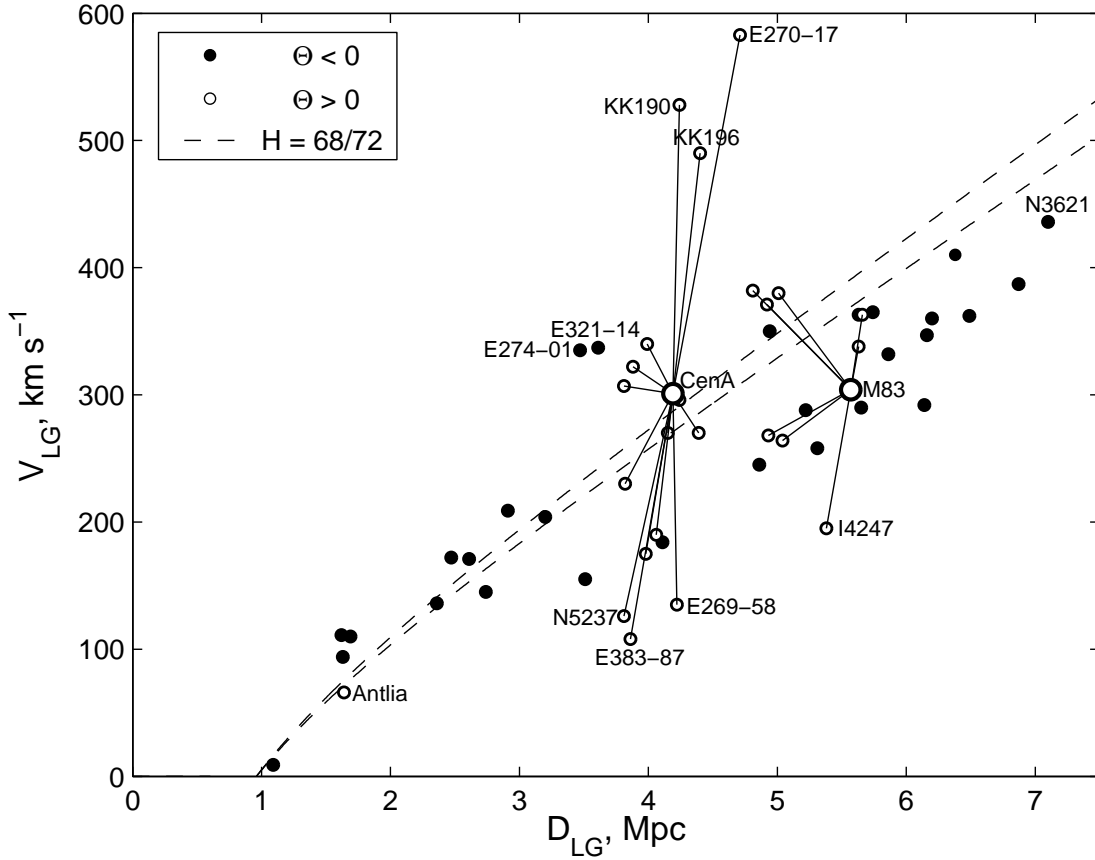


Fig. 8.— The Hubble diagram for galaxies in the Cen A/M 83 complex and its vicinity. Galaxies in groups ($\Theta > 0$) and in the general field ($\Theta < 0$) are indicated by open and filled circles, respectively. The companions to Cen A and M 83 are connected by lines to the main galaxies. The two dashed lines correspond to Hubble relations at $H_0 = 68$ and $72 \text{ km s}^{-1} \text{Mpc}^{-1}$.

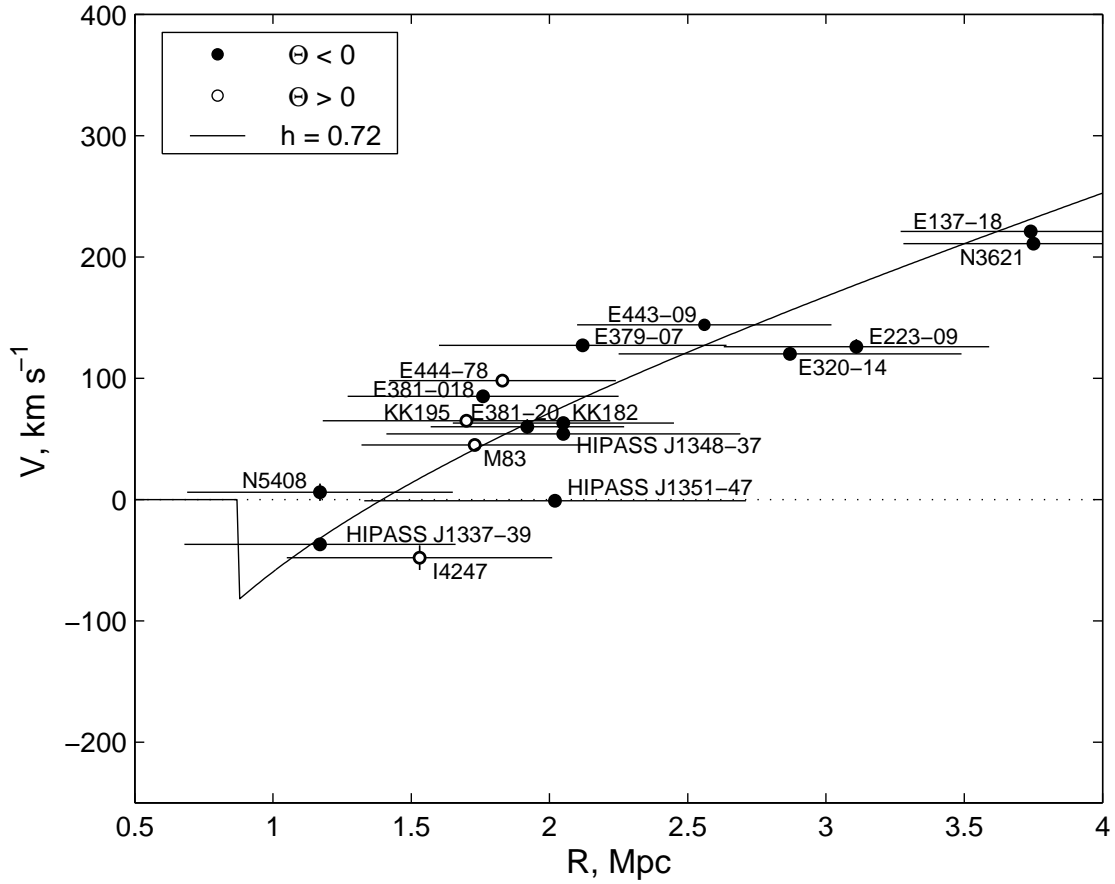


Fig. 9.— Distribution of the radial velocity difference and the spatial distance of galaxies with respect to the Centaurus A. Galaxies in groups and in the general field are indicated by open and filled circles, respectively.

Table 1: New distances to galaxies in the Cen A/M 83 complex

Name	RA(J2000.0)Dec	V_{LG}	I_{TRGB}	$(V-I)_{-3.5}$	A_I	μ_0	D	[Fe/H]
			σ_{TRGB}	σ_{V-I}		σ_{μ_0}		$\sigma_{[Fe/H]}$
E215–09, KKs40	105730.2–481044	290	24.98	1.55±0.006	0.43	28.60	5.25	–1.861
			0.07	0.21		0.16		0.024, 0.150
E320–14, KKs44	113753.4–391314	362	25.15	1.45±0.012	0.28	28.92	6.08	–1.923
			0.17	0.25		0.22		0.042, 0.154
E381–18	124442.7–355800	353	24.70	1.32±0.011	0.12	28.63	5.32	–2.059
			0.14	0.20		0.20		0.044, 0.162
E381–20	124600.4–335017	332	24.76	1.27±0.007	0.13	28.68	5.44	–2.343
			0.02	0.19		0.14		0.033, 0.177
E443–09, KK170	125453.6–282027	410	24.96	1.26±0.018	0.13	28.88	5.97	–2.435
			0.12	0.15		0.17		0.083, 0.181
KK182, Cen6	130502.9–400458	360	24.96	1.24±0.018	0.20	28.81	5.78	–2.741
			0.06	0.25		0.15		0.085, 0.196
E269–058	131032.9–465927	142	24.06	1.55±0.003	0.21	27.90	3.80	–1.431
			0.08	0.20		0.16		0.007, 0.122
KK189	131245.0–414955	–	24.40	1.47±0.012	0.22	28.23	4.42	–1.739
			0.07	0.13		0.16		0.042, 0.143
E269–66, KK190	131309.2–445324	528	24.04	1.62±0.005	0.18	27.91	3.82	–1.220
			0.04	0.20		0.15		0.014, 0.105
KK196	132147.1–450348	490	24.11	1.38±0.010	0.16	28.00	3.98	–1.961
			0.06	0.14		0.15		0.034, 0.156
KK197	132201.8–423208	–	24.19	1.69±0.006	0.30	27.94	3.87	–1.190
			0.04	0.16		0.15		0.017, 0.102
KKs55	132212.4–424351	–	24.21	1.49±0.006	0.28	27.98	3.94	–1.813
			0.03	0.11		0.14		0.036, 0.147
I4247, E444–34	132644.4–302145	195	24.55	1.25±0.008	0.12	28.48	4.97	–2.367
			0.15	0.23		0.21		0.034, 0.178
E444–78, UA365	133630.8–291411	363	24.65	1.39±0.005	0.10	28.60	5.25	–1.746
			0.10	0.16		0.17		0.023, 0.143
N5237	133738.9–425051	131	23.79	1.58±0.003	0.18	27.66	3.40	–1.330
			0.03	0.18		0.14		0.009, 0.114
KKs57	134138.1–423455	–	24.10	1.37±0.033	0.18	27.97	3.93	–1.630
			0.05	0.19		0.15		0.062, 0.136
CenN	134809.2–473354	–	24.10	1.52±0.012	0.27	27.88	3.77	–1.739
			0.04	0.13		0.15		0.035, 0.143
HIPASS1348–37	134833.9–375803	347	24.90	1.25±0.014	0.15	28.80	5.75	–2.519
			0.19	0.16		0.24		0.065, 0.186
E383–87	134918.8–360341	108	23.78	–	0.14	27.69	3.45	–
			–	–		–	–	–

Table 1: –Continued

Name	RA(J2000.0)Dec	V_{LG}	I_{TRGB} σ_{TRGB}	$(V-I)_{-3.5}$ σ_{V-I}	A_I	μ_0 σ_{μ_0}	D	[Fe/H] $\sigma_{[Fe/H]}$
HIPASS1351–47	135122.0–470000	292	25.02 0.22	1.36±0.014 0.20	0.28	28.79 0.26	5.73	–2.381 0.077, 0.179
E384–016	135701.6–352002	350	24.37 0.03	1.46±0.005 0.14	0.14	28.28 0.14	4.53	–1.622 0.015, 0.135
E223–09	150108.5–481733	387	25.51 0.07	1.69±0.004 0.32	0.50	29.06 0.16	6.49	–1.600 0.011, 0.134
E274–01	151413.5–464845	335	23.90 0.05	1.81±0.005 0.35	0.50	27.45 0.16	3.09	–1.217 0.008, 0.105
E137–18	162059.3–602915	421	25.45 0.06	1.60±0.005 0.36	0.47	29.03 0.16	6.40	–1.961 0.017, 0.156

Table 2. Galaxies in and around the Cen A/M 83 complex.

Galaxy name (1)	RA(J2000.0)Dec (2)	T (3)	Θ (4)	$V_{LG} \pm \sigma_V$ (5)	$D \pm \sigma_D$ (6)	Meth (7)	Ref (8)	Note (9)	
E059–01	073119.3–681110	9	–1.5	245	5	4.57	0.36	rgb	K06a
N2915	092611.5–763735	10	–1.3	184	5	3.78	0.43	rgb	CNG
SexB,DDO70	100000.1+051956	10	–0.7	111	1	1.36	0.07	rgb	CNG
N3109	100307.2–260936	9	–0.1	110	1	1.33	0.08	rgb	CNG
Antlia,P29194	100404.0–271955	10	2.3	66	0	1.28	0.13	rgb	T06
SexA,DDO75	101100.8–044134	10	–0.6	94	1	1.32	0.04	cep	CNG
E376–16	104327.1–370233	10		364	3	5.0		h	Ko04
P32250	104741.9–385115	7	–1.0	406	7	5.8		h	CNG
E215–09,KKs40	105730.2–481044	10	–0.9	290	2	5.25	0.41	rgb	K06b
N3621	111816.1–324842	7	–1.9	436	5	6.70	0.47	cep	CNG
HIPASS	113311.0–325743	10		414	5	5.8		h	M04
E320–14,KKs44	113753.4–391314	10	–1.2	362	5	6.08	0.65	rgb	K06b
E379–07,KK112	115443.0–333329	10	–1.3	363	5	5.22	0.52	rgb	CNG
E379–24	120456.7–354435	10		354	5	4.9		h	M04
E321–014	121349.6–381353	10	–0.3	337	5	3.19	0.26	rgb	CNG
I3104,E020–04	121846.1–794334	9	–0.5	171	5	2.27	0.19	rgb	CNG
KKs51	124421.5–425623	–3	0.7			3.6		mem	CNG C
E381–018	124442.7–355800	10	–0.6	365	1	5.32	0.51	rgb	K06b
E381–20	124600.4–335017	10	–0.3	332	6	5.44	0.37	rgb	K06b
HIPASS J1247–77	124732.6–773501	10	–1.0	155	3	3.16	0.25	rgb	K06a
E443–09,KK170	125453.6–282027	10	–0.9	410	1	5.97	0.46	rgb	K06b
E219–010	125609.6–500838	–3	0.1			4.28		sbf	CNG C
GR8,DDO155	125840.4+141303	10	–1.2	136	3	2.10	0.34	rgb	CNG
UA319	130214.4–171415	9	2.1	547	5	7.6		h	CNG
DDO161	130316.8–172523	8	1.4	545	5	7.6		h	CNG
E269–37,KK179	130333.6–463503	–3	1.6			3.48	0.35	rgb	CNG C
KK182,Cen6	130502.9–400458	10	–0.5	360	3	5.78	0.42	rgb	K06b
N4945	130526.1–492816	6	0.7	296	5	3.82	0.31	rgb	G05 C
P45628	130936.6–270826	10	–0.6	470	32	6.5		h	CNG
E269–058	131032.9–465927	10	1.9	135	3	3.80	0.29	rgb	K06b C
KKs53,Cen7	131114.2–385422	–3	1.2			3.6		mem	CNG C
KK189	131245.0–414955	–3	2.0			4.42	0.33	rgb	K06b C
E269–66,KK190	131309.2–445324	–1	1.7	528	31	3.82	0.26	rgb	K06b C
N5068	131855.3–210221	6	–1.4	473	5	6.6		h	CNG
KK195	132108.2–313147	10	0.0	338	5	5.22	0.52	rgb	CNG M

Table 2—Continued

Galaxy name (1)	RA(J2000.0)Dec (2)	T (3)	Θ (4)	$V_{LG} \pm \sigma_V$ (5)		$D \pm \sigma_D$ (6)		Meth (7)	Ref (8)	Note (9)
KKs54	132132.4–315311	–3	1.0			4.6		mem	CNG	M
KK196	132147.1–450348	10	2.2	490	5	3.98	0.29	rgb	K06b	C
N5102	132157.8–363747	1	0.7	230	7	3.40	0.39	rgb	CNG	C
KK197	132201.8–423208	–3	3.0			3.87	0.27	rgb	K06b	C
KKs55	132212.4–424351	–3	3.1			3.94	0.27	rgb	K06b	C
KK198	132256.1–333403	–3	0.8			4.6		mem	CNG	M
KK200	132436.0–305820	9	1.2	264	1	4.63	0.46	rgb	CNG	M
N5128,Cen A	132528.9–430100	–2	0.6	301	5	3.77	0.38	rgb	R04	C
I4247,E444–34	132644.4–302145	10	1.5	195	10	4.97	0.49	rgb	K06b	M
KK203	132728.1–452109	–3	2.1			3.6		mem	CNG	C
E324–24	132737.4–412850	10	2.4	270	6	3.73	0.43	rgb	CNG	C
P170257	132921.0–211045	10	0.2	457	29	6.3		h	CNG	
N5206	133343.9–480904	–3	1.1	322	10	3.47	0.28	rgb	Sh06	C
E270-17,RFGC2603	133447.3–453251	8	1.0	583	2	4.3	0.8	tf	K06b	C
E444–78,UA365	133630.8–291411	10	2.1	363	1	5.25	0.43	rgb	K06b	M
KK208	133635.5–293415	–3	1.6			4.68	0.46	rgb	CNG	M
N5236, M83	133700.1–295204	5	0.8	304	4	5.16	0.41	rgb	K06b	M
DEEP J1337–33	133700.6–332147	10	1.2	371	5	4.51	0.45	rgb	CNG	M
E444–84	133720.2–280246	10	1.7	380	4	4.61	0.46	rgb	CNG	M
HIPASS J1337–39	133725.1–395352	10	–0.3	258	5	4.90	0.49	rgb	CNG	
N5237	133738.9–425051	–3	2.1	126	5	3.40	0.23	rgb	K06b	C
N5253	133955.8–313824	8	0.0	190	4	3.60	0.20	rgb	Sa04	C
I4316,E445–06	134018.1–285340	10	2.4	382	12	4.41	0.44	rgb	CNG	M
N5264	134137.0–295450	10	2.6	268	3	4.53	0.45	rgb	CNG	M
KKs57	134138.1–423455	–3	1.8			3.93	0.28	rgb	K06b	C
KK211	134205.6–451218	–5	1.5	340	23	3.58	0.36	rgb	CNG	C
KK213	134335.8–434609	–3	1.7			3.63	0.36	rgb	CNG	C
E325–11	134500.8–415132	10	1.1	307	4	3.40	0.39	rgb	CNG	C
KKs58	134600.8–361944	–3	0.6			3.6		mem	CNG	C
KK217	134617.2–454105	–3	1.1			3.84	0.38	rgb	CNG	C
KK218	134639.5–295845	–3	1.6			4.6		mem	CNG	M
E174–01,KKs59	134757.7–532104	10	–1.5	432	6	6.0		h	CNG	
CenN	134809.2–473354	–3	0.9			3.77	0.26	rgb	K06b	C
HIPASS J1348–37	134833.9–375803	10	–1.2	347	3	5.75	0.66	rgb	K06b	
KK221	134846.4–465949	–3	0.6	270	33	3.98	0.40	rgb	CNG	C

Table 2—Continued

Galaxy name (1)	RA(J2000.0)Dec (2)	T (3)	Θ (4)	$V_{LG} \pm \sigma_V$ (5)	$D \pm \sigma_D$ (6)	Meth (7)	Ref (8)	Note (9)		
E383–87	134918.8–360341	8	0.5	108	1	3.45	0.27	rgb	K06b	C
HIPASS J1351–47	135122.0–470000	10	–1.1	292	3	5.73	0.73	rgb	K06b	
KKH86	135433.6+041435	10	–1.5	209	3	2.61	0.16	rgb	CNG	
E384–016	135701.6–352002	10	–0.3	350	32	4.53	0.31	rgb	K06b	
N5408	140321.5–412235	10	–0.5	288	7	4.81	0.48	rgb	CNG	
Circinus,E97–13	141309.3–652021	3	–0.7	204	10	2.82	0.28	tfi	K06b	
DDO187	141556.5+230319	10	–1.3	172	4	2.28	0.23	rgb	T06	
P51659	142803.7–461806	10	0.1	175	2	3.58	0.33	rgb	CNG	C
E222–10	143503.0–492518	10	–1.4	405	5	5.8		h	CNG	
HIPASS	144127.0–624155	10		441	3	6.1		h	M04	
E272–25	144325.5–444219	8	–1.5	422	10	5.9		h	CNG	
E223–09	150108.5–481733	10	–0.8	387	6	6.49	0.51	rgb	K06b	
E274–01	151413.5–464845	7	–0.8	335	5	3.09	0.23	rgb	K06b	
HIPASS J1526–51	152617.0–511004			416		5.8		h	M04	
E137–18	162059.3–602915	9	–1.8	420	3	6.40	0.48	rgb	K06b	
I4662,E102–14	174706.3–643825	9	–0.9	145	4	2.44	0.19	rgb	K06a	
Tucana,P69519	224149.0–642512	–2	–0.1	9	2	0.88	0.09	rgb	CNG	

Table 3: Total mass estimates for the extended halo of Cen A.

Method	Scale kpc	M_{tot} $10^{12}M_{\odot}$	Reference
Globular clusters	45	0.8 – 1.8	Woodley 2006
Planetary Nebulae	80	0.5 – 0.6	Peng et al. 2004
Orbital/virial	400	6.4 – 8.1	present paper
Turn-over radius with $\Omega_m = 0.27$	1400	4.4 – 7.3	present paper
Typical lensing mass for given L	500	2.4 – 5.2	Hoekstra et al. 2005